DETERMINATION OF TERTIARY CELLS IN A VERTICAL SLOT

Pedro F. de Abreu
Computer Engineering Department, Vale do Itajaï University – UNIVALI and
Computational Fluid Dynamics Laboratory, Federal University of Santa Catarina
88.040-900 – Florianópolis – SC – Brazil

Roydon A. Fraser, John L. Wright
Mechanical Engineering Department, University of Waterloo
Waterloo – ON – Canada – N2L 3G1

Clovis R. Maliska
Computational Fluid Dynamics Laboratory – SINMEC
Federal University of Santa Catarina
88.040-900 – Florianópolis – SC – Brazil

SUMMARY

A procedure that allows the formation of tertiary cells as low as the theoretical critical Rayleigh number, Ra_t, using central differencing scheme (CDS) without a use of a higher scheme was devised. The numerical results are compared with experimental results and with the only numerical solution reported in the literature. It is well known that second and first order schemes preclude the generation of secondary cells at the Ra_c. Knowing that two or more solutions exist at lower Ra, it was thought that the simulation might select a solution with secondary and tertiary cells if it were given a "push", i.e., overriding the delay effect introduced by the discretization scheme, by perturbing the flow by summing the existing flow field with a "perturbation" velocity field which resembles secondary cells and tertiary cells. The flow is modeled for a range of Prandtl number, Pr, of 50 to 1000, to compare with the results reported in the literature. Also, to justify the discrepancies between the numerically simulated and measured Nusselt Numbers, Nu, for $Ra > 1.4 \times 10^4$ in air a try was done for Pr as low as 0.71. Although the procedure has been shown to be able to model tertiary cells for $Pr \geq 50$ near the critical Rayleigh number for tertiary cells, Ra_t, it is not able to do the same for $Pr = 0.71$ (air). Therefore, it can be concluded that tertiary flows do not exist for air Prandtl number ($Pr = 0.71$), or that any tertiary flow in the cavity is so weak that this procedure is not able to reproduce it. It is more likely the flow is going to transition to turbulence.

INTRODUCTION

The motivation of this work, the determination of tertiary cells in a vertical slot, arose when a literature survey in tall cavities was done by de Abreu (1996) to employ the state of the art in modeling complex fenestration systems (windows). It was found, see Figure 1, that for air, Pr=0.71, cavity aspect ratio, A=40, Rayleigh number, $Ra>1.4\times10^4$, the numerically calculated values of Nusselt Numbers, Nu, with secondary flow being modeled by Raithby and Wong (1981), Lee and Korpela (1983), Wright (1990), were lower than those measured by ElSherbiny *et al.* (1982) and Shewen(1986). Consequently, the simulation was not fully modeling all of the physical mechanisms of heat transfer. This discrepancy could be due to, among several factors, the presence of tertiary cells, the appearance of unsteady cat's eyes and three dimensional effects which would increase the heat transfer. Although tertiary flows have only been visualized in oil by Elder (1965), Seki *et al.* (1978a and 1978b), Chen and Thangam (1985) and Wakitani (1994) and numerically determined for $Pr > 50$ by de Vahl Davis and Mallinson (1975), they were modeled for air in this work to verify whether they are present in the flow in range of the critical Rayleigh number.

The reason for perturbing the tertiary cells is because in that range neither the experiments of ElSherbiny *et al.* (1982) nor Shewen (1986) have shown unsteady disturbance, and no work has been done to determine tertiary cells for Pr as low as for air. Also, the first appearance of the tertiary flow in the work of de Vahl Davis and Mallinson (1975) was far from the experimental critical Rayleigh number, Ra_t.

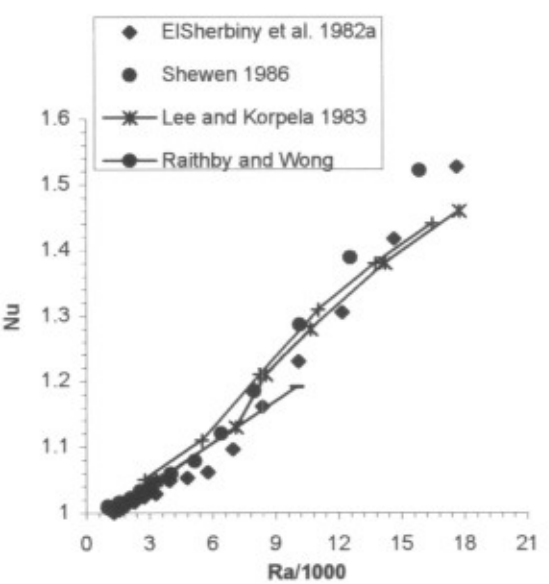

Figure 1: Comparison of Available Simulation and Measured *Nu vs. Ra* Results for the Vertical Cavity, A=40.

At high Rayleigh numbers, $Ra > Ra_c$, transverse stationary cells may be expected. For $A = 40$, Wright (1990) and de Abreu (1996) have shown that if secondary cells are not modeled in the flow, the heat transfer across the cavity, for $Ra > Ra_c$, is lower than the measured values of ElSherbiny *et al.* (1982) and Shewen (1986). When the secondary cells are generated the values for the heat transfer across the cavity agree with those measured within 1% to 5%.

Several models have been able to resolve secondary cells in the vertical cavities (Roux *et al.*, 1979; Korpela *et al.*, 1982; Lee and Korpela, 1983; de Vahl Davis and Jones, 1984; Chait and Korpela, 1989; Ramanan and Korpela, 1989; Le Queré, 1990). It is well known (Patankar, 1980) that fully upwind differencing schemes (UDS) or hybrid schemes, as exponential differencing schemes, EDS, produce false diffusion in recirculating flows which may overwhelm the physical diffusion when convection effects are dominant. This effect can delay the onset of the instabilities. This might be true when tertiary cells appear.

Most models capable of generating secondary cells, near the critical Rayleigh number, are based on high order discretization schemes (Roux *et al.*, 1979; Korpela *et al.*, 1982; Ramanan and Korpela, 1989; Chait and Korpela, 1989; Le Queré, 1990). Due to the difficulty of applying the method, boundary conditions and solving the conjugate problem they are not suitable to solve the window problem. Others claim to have avoided false diffusion by using a central differencing scheme (CDS) and uniform grids (Lauriat and Desrayaud, 1985; de Vahl Davis and Jones, 1984; Wright, 1990), but only Wright (1990) could obtain secondary cells near the critical Rayleigh number. Although from the results of the stability analysis of Bergholz (1978), the secondary cells might be expected for *Ra* as low as 7,150 for $A = 20$, de Vahl Davis and Jones (1984) and Lauriat and Desrayraud (1985) have reported secondary cells for *Ra* as low as 2×10^4 and 2.2×10^4, respectively. However, Wright (1990) , perturbing the flow, has modeled secondary cells with *Ra* as low as the theoretical critical value. The numerical model employed here uses the same approach used by Wright (1990), CDS when secondary or tertiary cells are expected and EDS when they are not expected.

NUMERICAL MODEL

Obtaining solutions to the nonlinear Navier-Stokes equations has always been a challenge to fluid mechanicians and mathematicians alike. Even though exact solutions do exist (Schlichting, 1979), they are restricted to very specialized cases. Much of the effort has therefore been devoted to developing approximate solution techniques which can be applied to a much larger variety of problems.

For the natural-convection phenomena in cavities, as described by Equations (1), (2), (3), and (4), the momentum and energy equations are coupled through the body force term which depends on the temperature field. As a result, all the aforementioned equations must be solved simultaneously and hence represent an additional level of complexity to obtaining a solution.

- **continuity**:

$$\frac{\partial u}{\partial x} + \frac{\partial v}{\partial y} = 0 \qquad (1)$$

- **momentum**:

in x:

$$\rho \frac{Du}{Dt} = -\frac{\partial p_k}{\partial x} + \mu \left(\frac{\partial^2 u}{\partial x^2} + \frac{\partial^2 u}{\partial y^2} \right) \qquad (2)$$

in y:

$$\rho \frac{Dv}{Dt} = -\frac{\partial p_k}{\partial y} + \mu \left(\frac{\partial^2 v}{\partial x^2} + \frac{\partial^2 v}{\partial y^2} \right) + \rho g \beta \left(T - \overline{T} \right) \qquad (3)$$

- **energy**:

$$\rho c_p \frac{DT}{Dt} = k \left(\frac{\partial^2 T}{\partial x^2} + \frac{\partial^2 T}{\partial y^2} \right) + \dot{S} \qquad (4)$$

where, ρ, μ, β, g, c_p and k are the density, viscosity, coefficient of thermal expansion, gravity, constant-pressure specific heat and conductivity, respectively; t is the time; x, y are the Cartesian coordinates; u, v are the velocity components; T is the temperature; $\rho g \beta (T - \overline{T})$ is the buoyancy force/unit volume in the y direction where $\overline{T} = (T_h + T_c)/2$; T_h and T_c are the temperatures at the hot wall and cold wall, respectively; $\dot{S}$ is the source term, and the origin of the coordinates (x, y) is placed at the most lower left corner of the cavity with gravity in the $-y$ direction. p_k, the kinematic pressure, drives the flow. It is obtained from the following expression

$$p(y) = p_o - \int_0^y \overline{\rho}(y) g \, dy + p_k$$

A Finite Volume Method (FVM) (Patankar, 1980) using a collocated pressure arrangement on a non-orthogonal grid (Rhie, 1981) was used in this work. In this formulation the approximate equations are obtained through conservation balances of the conserved property (mass, momentum, enthalpy, etc.) in the elemental control volume.

Equation Discretizations. Heat transfer and fluid flow problems require the solution of general conservation equations (Patankar, 1980) of the form

$$\frac{\partial}{\partial t}(\rho \Phi) + \frac{\partial}{\partial x}(\rho u \Phi) + \frac{\partial}{\partial y}(\rho v \Phi) = \frac{\partial}{\partial x}\left(\Gamma^{\Phi} \frac{\partial \Phi}{\partial x} \right) + \frac{\partial}{\partial y}\left(\Gamma^{\Phi} \frac{\partial \Phi}{\partial y} \right) + \dot{S}^{\Phi} \qquad (5)$$

over some specified problem domain and with the appropriate boundary conditions for the solution variable which may represent any conserved quantity.

The collocated grid formulation that was implemented (Rhie, 1981) is applied over each control volume, as depicted in Figure 2. Each rectangular control volume whose node is designated as P, has four neighboring nodes designated by their compass bearing from P, i.e., S, N, W and E; similarly, s, n, w and e refer to the location of the faces of the control volume of interest. Δx_w and Δx_e are the distances in the x direction from the node to the west and east faces of the control volume considered, respectively, while Δy_s and Δy_n are the distances to the south and north faces, respectively. The variables p, u, v and T are located and calculated at the center of the P control volumes.

The transport equations are integrated over a finite number of control volumes (CVs), leading to balance equations of fluxes J through the CV faces, and volumetric sources $\dot{S}^{\Phi}$.

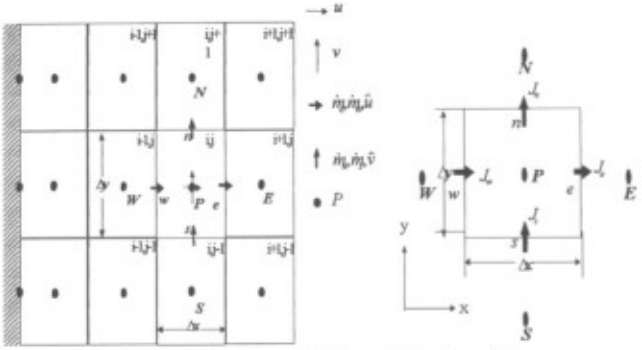

Figure 2: Computational Grid and Labeling Scheme.

Thus

$$J_e - J_w + J_n - J_s = 0 \tag{6}$$

Evaluation of the convection and diffusion contribution to the flux J will be described for the CV face "e". Analogous expressions follow for the others faces.

First the cell face mass flux is evaluated as

$$\dot{m}_e = \rho \hat{u} A_e \tag{7}$$

where $\hat{u}$ is the convecting velocity in the x direction. The mass fluxes are assumed to be known when solving the momentum and heat transport equations.

The convective flux of a variable Φ is evaluated as

$$J_e^c = \dot{m}_e \Phi_e \tag{8}$$

where Φ_e stands for the mean value of the transported variable (u, v *or* T) at CV face "e". The estimate for this value is expressed in terms of the nodal values by employing the upwind weighted scheme of Raithby and Torrance (1974), from now on called EDS (Exponential Differencing Scheme).

The diffusion flux involves an estimate of the mean gradient of Φ at the CV face. Here again EDS is employed, leading to

$$J_e^D = -\Gamma \left.\frac{\partial \Phi}{\partial n}\right|_e A_e \tag{9}$$

To perform the integration, values of variables at the faces of the control volumes were related to the nodal values using EDS. Hence, to relate Φ_e to Φ_E and Φ_P, the following approximation is made:

$$\Phi_e = (0.5 + \alpha_e)\Phi_P + (0.5 - \alpha_e)\Phi_E \tag{10}$$

Furthermore, the diffusion at the east face is approximated by:

$$\Gamma_e \left.\frac{\partial \Phi}{\partial n}\right|_e = \beta_e \frac{\Gamma_e}{\Delta x}(\Phi_E - \Phi_P) \tag{11}$$

The convective and diffusive weights, α_e and β_e, are functions of the Peclet number, Pe, i.e.:

$$\alpha_e = 0.5\left(\frac{Pe^2}{5 + Pe^2}\right)\frac{|\dot{m}_e|}{\dot{m}_e} \tag{12}$$

$$\beta_e = \frac{1 + 0.005 Pe^2}{1 + 0.05 Pe^2} \tag{13}$$

where $Pe = \dfrac{\dot{m}_e}{D_e}$, $D_e = \dfrac{\Gamma_e A_e}{\Delta x}$, $\dot{m}_e$ is the mass flux through the east face, A, is the surface area of the east face, and Δx is the distance in the x direction between nodes P and E.

After integration is performed using the EDS scheme, the resulting equation is an algebraic expression of the form:

$$A_P^\Phi \Phi_P = A_N^\Phi \Phi_N + A_S^\Phi \Phi_S + A_E^\Phi \Phi_E + A_W^\Phi \Phi_W + B^\Phi \tag{14}$$

Equation. (14) can be cast in a short form:

$$A_p^\Phi \Phi_p = \sum A_{nb}^\Phi \Phi_{nb} + B^\Phi \tag{15}$$

where the subscript *nb* refers to the nodes neighboring node P, i.e., W, E, S and N. In Equation. (14), the A's are the coefficients and B^Φ is the source term:

$$\begin{aligned}
A_N^\Phi &= \beta_n D_n - \frac{\dot{m}_n}{2} + \alpha_n \dot{m}_n \\
A_S^\Phi &= \beta_s D_s + \frac{\dot{m}_s}{2} + \alpha_s \dot{m}_s \\
A_E^\Phi &= \beta_e D_e - \frac{\dot{m}_e}{2} + \alpha_e \dot{m}_e \\
A_W^\Phi &= \beta_w D_w + \frac{\dot{m}_w}{2} + \alpha_w \dot{m}_w \\
A_P^\Phi &= A_N^\Phi + A_S^\Phi + A_E^\Phi + A_W^\Phi - R^\Phi \mathcal{V} + \frac{M_P}{\Delta t} \\
B^\Phi &= Q^\Phi \mathcal{V} + \frac{M_P^0 \Phi_P^0}{\Delta t} \\
M_P &= \rho \mathcal{V}
\end{aligned} \tag{16}$$

For a value of grid Peclet number greater than ten, $|\mathrm{Pe}| \geq 10$, the exponential scheme (EDS) approaches the fully upwind differencing scheme (UDS). If the grid Peclet number is smaller than two, $|\mathrm{Pe}| \leq 2$, it approaches the central difference scheme (CDS). So to use UDS, the values of the convective and diffusive weights should be set constant, say, α=0.5 and β=0.1, and to apply CDS , the values of the convective and diffusive weights should be fixed to, α=0 and β=1.

Grid Description. The aim of the finite volume method is to replace Equation (5) with a set of algebraic equations involving the values of Φ at a finite number of discrete control volumes and to preserve conservation throughout. Uniform grid spacings in both the x and y directions are used in the cavity because secondary cells can be present in the flow and can be present everywhere. This precludes the use of a non-uniform grid.

Since false diffusion depends on the control volume size, it is expected that different false diffusion levels would lead to different solutions (Markatos and Pericleous, 1984). To obtain high resolution in the computed results and ensure good accuracy without the contamination of false diffusion, the control volume sizes should be as small as possible, though not so small as to overtax the available computing facilities. As pointed out by Wright (1990) the grid aspect ratios (i.e., $A_{grid} = \Delta y/\Delta x$) used in the studies found in the literature (Raithby and Wong, 1981; Korpela *et al.*, 1982; Lee and Korpela, 1983; Ramanan and Korpela, 1989) ranged from 2.5 to 10. Throughout the current study the grid aspect ratio will be 5.

Perturbation. To model secondary cells, the same four step procedure used by Wright (1990) will be utilized, as follow:

1) establish the solution for a unicellular base flow using EDS, allowing large time step;
2) switch to CDS, reducing the time step to the maximum explicit time step;
3) perturb the flow by summing the existing flow field with a "perturbation" velocity field which resembles secondary cells alone and;
4) allow the iteration process to continue to convergence.

The perturbation field is generated following the steps below given by Wright (1990).

The height of a single secondary cell, l_c, expressed in terms of a wave-number, α_c, and width of the cavity, l, is

$$l_c = l\left(\frac{2\pi}{\alpha_c}\right) \tag{17}$$

where α_c is the interpolated value between the wave-numbers given in Lee and Korpela (1983). These are:

α_c=2.82 Gr=1.1x10^3

α_c=2.50 Gr=1.5x10^3

α_c=2.41 Gr=2.0x10^3

α_c=2.33 Gr=2.5x10^3

and $Ra = Pr \cdot Gr$. If $Gr < 1.1\text{x}10^3$, α_c, is set to 2.82.

The number of cells, n_c, is

$$n_c = INT\left[(A-10)\frac{\alpha_c}{2\pi}\right] + 2 \tag{18}$$

and the perturbation velocity components at the P point of the any control volume, u_c and v_c, are:

$$u_c = \frac{u_{max}}{\alpha_c A}(\Psi_S - \Psi_N) \bullet (je - jb + 1) \tag{19}$$

$$v_c = \frac{u_{max}}{\alpha_c}(\Psi_E - \Psi_W) \bullet (ie - ib + 1) \tag{20}$$

where the perturbation stream function, Ψ_c, is applied over the solution grid and scaled such that the maximum value of u_c would be half of the maximum value of u known in the unicellular base flow, u_{max}. This scaling differs slightly from that presented by Wright (1990), where he used $u_c \le u_{max}$. The reason for this difference is that the secondary flow is weaker than the unicellular base flow, so the velocities must be lower in the secondary flow than in the unicellular base flow which leads to a faster convergence.

The perturbation stream function (Wright, 1990) is given by

$$\Psi_c = -\frac{1}{2} \bullet \left(1 + \cos\left(2\pi\left(\frac{x}{l} - \frac{1}{2}\right)\right)\right) \bullet \left(1 - \cos\left(\alpha_c A\left(\frac{y}{h} - \frac{1}{2}\right) + n_{o/e}\pi\right)\right) \tag{21}$$

where $n_{o/e}$=1 if n_c is odd, $n_{o/e}$=0 if n_c is even.

Equation (21) applies over the range

$$\frac{(h - n_c l_c)}{2} < y < \frac{(h + l_c n_c)}{2} \tag{22}$$

Otherwise, near the ends of the cavity, $\Psi_c = 0$.

The procedure to generate the perturbation field for the tertiary flow will be similar to that producing the perturbation field for the secondary flow:

1) calculate l_c and n_c for the secondary flow;
2) find the number of tertiary cells , n_t=n_c-1. Here, the assumption is made that between two secondary cells there is one tertiary cell;
3) determine the new height of a single secondary cell, l_{cn} and the height of the tertiary cell, l_t. The l_{cn} was thought to be 2.5 times l_t, because this was the scaling found by both Elder (1965) and Seki *et al.* (1978a and 1978b) in their visualization experiments;
4) estimate the perturbation stream function,

where,

$$l_{cn} = 2.5 l_t \quad and \quad l_t = \frac{l_c}{\left(3.5 + \frac{1}{n_c}\right)} \tag{23}$$

$$\Psi_c = -\left(1 + \cos\left(2\pi\left(\frac{x}{l} - \frac{1}{2}\right)\right)\right) \bullet \left(1 + \cos\left(2\pi\left(\frac{y^*}{l_{st}} - \frac{1}{2}\right)\right)\right) \bullet (-1)^n \tag{24}$$

and

$$y^* = y - \left(\frac{1}{2}(h - n_c l_c) + n_{ts} l_{cn} + n_{tt} l_t\right) \tag{25}$$

n_{ts}, n_{tt} are the number of times the secondary cells and tertiary cells were generated, n=n_{ts}+n_{tt} and l_{st} is equal to l_{cn} or l_t depends on the cell that are being produced. The generation of the stream function for the secondary and tertiary cells alternates between the two. First a secondary, and then a tertiary cell is generated, then a secondary cell, and so on, until the last secondary cell is made;

5) evaluate the perturbation velocity components of the tertiary cells. The maximum velocities for the perturbation field of the tertiary flow were supposed to be 5 times less than that of the secondary flow, because the tertiary flow is weaker,

$$u_t = \frac{u_{max}}{5\alpha_c A}(\Psi_S - \Psi_N) \bullet (je - jb + 1) \tag{26}$$

$$v_t = \frac{u_{max}}{5\alpha_c}(\Psi_E - \Psi_W) \bullet (ie - ib + 1) \tag{27}$$

RESULTS

To examine the reliability of the code to generate tertiary cells near the critical Rayleigh number comparison with experiments and numerical results are presented

A grid size study was conducted on computational meshes ranging from 10 to 40 control volumes in the horizontal direction, with grid (cell) aspect ratio 5, cavity aspect ratio 10, 15 and 20, Pr = 0.71 for Ra = 10^4 and, Pr = 100 for Ra = 10^5. For these different grids the difference in total heat transfer to the warm wall and the maximum velocities and temperature is less than 1% for all cases for a grid consisting of 30 and 40 control volumes. Therefore, the grid with 30 control volumes in the horizontal direction for any aspect ratio cavity was selected for the calculations unless otherwise noted. The nodes are regularly spaced in

order to assist capturing the secondary cells when present. It is noticed that the grid is fine enough to resolve the thermal and velocity boundary layers near the wall when they are present.

It was seen in the introduction that for $Ra > 1.4 \times 10^4$ the calculated values of Nusselt Numbers, Nu, are lower than those measured by ElSherbiny *et al.* (1982) and Shewen (1986) (see Figure 1). Consequently, the simulation is not fully modeling all of the physical mechanisms of heat transfer. Among several factors that could increase the heat transfer are the presence of tertiary cells, the appearance of unsteady cat's eyes and three dimensional effects. Although tertiary flows have only been visualized in oil by Elder (1965), Seki *et al.* (1978a and 1978b), Chen and Thangam (1985) and Wakitani (1994) and numerically determined for $Pr = 1000$ by de Vahl Davis and Mallinson (1975), they are modeled in this work to verify whether they are present in the Rayleigh number flow of windows and for air. The reason tertiary cells are suspected is because in this range neither the experiments of ElSherbiny *et al.* (1982) nor Shewen (1986) have shown unsteady disturbances, and no work has been done to determine the regime for tertiary cells for Pr number as low as that for air. Also, the first appearance of tertiary flow in the work of de Vahl Davis and Mallinson (1975) was far from the experimental critical Ra_t (they did not use any provision to perturb the flow). Table 1 summarizes the aforementioned results and the results of this work. For $Pr = 900$ the Ra_t found using the simple model presented here was 8.9×10^5 which is near of expected value Ra_t, within experimental error presented by Wakitani (1994), $8.5 \times 10^5 \pm 10\%$.

Works	Pr	A	Ra_t
Elder (1965)	1000	10-20	$3.0\ Ra_c$
Seki et al. (1978b)	480	15	3.0×10^5
Chen and Thangam (1985)	160	15	$2.5\ Ra_c$
Wakitani (1994)	50	15	1.7×10^6
	125	10	1.0×10^6
	125	15	1.8×10^6
	900	10	8.5×10^5
de Vahl Davis and Mallinson (1975)	1000	10	9.4×10^5
Present work	55	15	1.8×10^6
	125	15	1.9×10^6
	793	10	8.9×10^5
	900	10	8.9×10^5

Table 1: Summary of Values for Critical Rayleigh Number for Onset of Tertiary Flow.

To verify the existence of tertiary flow in a cavity filled with air, the flow was perturbed by superimposing a tertiary flow, in the range of Rayleigh numbers, $1.5 \times 10^4 < Ra < 2.0 \times 10^4$. For this range of Ra the cells perturbed die out in the course of converging to a solution.

CONCLUSIONS

Although the model presented here has been shown to be able to model tertiary cells for $Pr \geq 50$ near the critical Rayleigh number for tertiary cells, Ra_t, it is not able to do the same for $Pr = 0.71$ (air). Therefore, it can be concluded that tertiary flows does not exist for air Prandtl number ($Pr = 0.71$), or that any tertiary flow in the cavity is so weak that this model is not able to reproduce it. It is more likely the flow is going to transition to turbulence. Seki *et al.* (1978b) in their visualization experiments pointed out that when tertiary cells appear, which is created by shear stress between two secondary cells, does not increase substantially the heat flow between the two vertical walls in contrast to when the flow changes to transition type flow. Consequently, further work has to be done to determine the reasons for the existing discrepancies between numerical and experimental results for high Ra in air

REFERENCES

Bergholz, R. F., 1978. "Instability of Steady Natural Convection in a Vertical Fluid Layer", Journal of Fluid Mechanics, vol. 84(4), pp. 743-768.

Chait, A. and S.A. Korpela, 1989. "The Secondary Flow and Its Stability for Natural Convection in a Tall Vertical Enclosure", Journal of Fluid Mechanics, vol. 200, pp. 189-216.

Chen, C.F. and S. Thangam, 1985. "Convective Stability of a Variable Viscosity Fluid in a Vertical Slot", Journal of Fluid Mechanics, vol. 161, pp. 161-173.

de Abreu, P.F., 1996. "Modeling the Thermal Performance of Windows Using a Two-Dimensional Finite Volume Model," Ph.D. Thesis, Department of Mechanical Engineering, University of Waterloo.

de Vahl Davis, G. and I.P. Jones, 1984. "The Effect of Vertical Temperature Gradients on Multi-Cellular Flows in High Aspect Ratio Cavities". In Proceedings of the Conference on Liquid Metal Technology in Energy Production, Oxford, April 9-13.

de Vahl Davis, G. and G.P Mallison, 1975. "A note on Natural Convection in a Vertical Slot", Journal of Fluid Mechanics, vol. 72(1), pp. 87-93.

Elder, J.W., 1965. "Laminar Free Convection in a Vertical Slot", Journal of Fluid Mechanics, vol. 23(1), pp. 77-98.

ElSherbiny, S.M., G.D. Raithby and K.G.T. Hollands, 1982. "Heat Transfer by Natural Convection Across Vertical and Inclined Air Layers", Journal of Heat Transfer, vol. 104, pp. 96-102.

Korpela, S.A., Y. Lee and J.E. Drummond, 1982. "Heat Transfer Through a Double Pane Window", Journal of Heat Transfer, vol. 104, pp. 539-544.

Lauriat, G. and G. Desrayaud, 1985. "Natural Convection in Air-Filled Cavities of High Aspect Ratios: Discrepancies Between Experimental and Theoretical Results", presented at the National Heat Transfer Conference, ASME, Denver, Colorado, August 4-7.

Le Queré, P., 1990. "A Note on Multiple and Unsteady Solutions in Two-Dimensional Convection in Tall Cavity", Journal of Heat Transfer, vol. 112, pp. 965-974.

Lee, Y. and S.A. Korpela, 1983. "Multicellular Natural Convection in a Vertical Slot", Journal of Fluid Mechanics, vol. 126, pp. 91-121.

Markatos, N.C. and K.A. Pericleous, 1984. "Laminar and Turbulent Natural Convection in a Enclosed Cavity", International Journal of Heat and Mass Transfer, vol. 27, pp. 755-772.

Patankar, S.V., 1980. "Numerical Heat Transfer and Fluid Flow", Hemisphere Publishing Corp.

Raithby G.D. and K.E. Torrance, 1974. "Upstream-Weighted Differencing Schemes and their Application to Elliptic Problems Involving Fluid Flow", Computer & Fluids, vol. 2, pp. 191-206.

Raithby, G.D. and H.H. Wong, 1981. "Heat Transfer by Natural Convection Across Vertical Air Layers", Numerical Heat Transfer, vol. 4, pp. 447-457.

Ramanan, N. and Korpela, S.A., 1989. "Multigrid Solution of Natural Convection in a Vertical Slot", Numerical Heat Transfer, vol. 15(3), part A, pp. 323-339.

Rhie, C.M., 1981. "A Numerical Study of the Flow Past an Isolated Aerofoil with Separation", Ph.D. Thesis, University of Illinois, Champaign, Urbana, chap. 4, pp. 22-35.

Roux, B., J-C. Grondin and P. Bontoux, 1979. "Natural Convection in Inclined Rectangular Cavities", Proceedings of the 1st International Conference on Numerical Methods in Thermal Problems, pp. 423-432, July 2-6.

Schlichting, H., 1979. "Boundary-Layer Theory", McGraw-Hill Publishing Company.

Seki, N., S. Fukusako and H. Inaba, 1978a. "Visual Observation of Natural Convective Flow in a Narrow Vertical Slot", Journal of Fluid Mechanics, vol. 84(4), pp. 695-704.

Seki, N., S. Fukusako and H. Inaba, 1978b. "Heat Transfer of Natural Convection in a Rectangular Cavity with Vertical Walls of Different Temperatures", Bulletin of the JSME, vol. 21, pp. 246-253.

Shewen, E.C., 1986. "A Peltier-Effect Technique for Natural Convection Heat Flux Measurement Applied to the Rectangular Open Cavity", Ph.D. Thesis, Department of Mechanical Engineering, University of Waterloo.

Wakitani, S., 1994. "Experiments on Convective Instability of Large Prandtl Number Fluids in a Vertical Slot", Journal of Heat Transfer, vol. 116(1), pp. 120-126.

Wright, J.L., 1990. "The Measurement and Computer Simulation of Heat Transfer in Glazing Systems," Ph.D. Thesis, Department of Mechanical Engineering, University of Waterloo.